The Reverse Warburg Effect and ^{18}F-FDG Uptake in Non–Small Cell Lung Cancer A549 in Mice: A Pilot Study

Guojian Zhang*[1,2], Jianbo Li*[1,2], Xuemei Wang[1], Yuanyuan Ma[3], Xindao Yin[2,4], Feng Wang[4], Huaiyu Zheng[2], Xiaoxian Duan[2], Gregory C. Postel[2], and Xiao-Feng Li[2]

[1]Department of Nuclear Medicine, Inner Mongolia Medical University Affiliated Hospital, Hohhot, Inner Mongolia, China; [2]Department of Diagnostic Radiology, University of Louisville, Louisville, Kentucky; [3]Department of Pathology, Memorial Sloan Kettering Cancer Center, New York, New York; and [4]Department of Radiology, Nanjing First Hospital, Nanjing Medical University, Nanjing, Jiangsu, China

The purpose of this study was to observe the effect of fasting and feeding on ^{18}F-FDG uptake in a mouse model of human non–small cell lung cancer. **Methods:** In in vivo studies, ^{18}F-FDG small-animal PET scans were acquired in 5 mice bearing non–small cell lung cancer A549 xenografts on each flank with continuous feeding and after overnight fasting to observe the changes in intratumoral distribution of ^{18}F-FDG and tumor ^{18}F-FDG standardized uptake value (SUV). In ex vivo studies, intratumoral spatial ^{18}F-FDG distribution assessed by autoradiography was compared with the tumor microenvironment (including hypoxia by pimonidazole and stroma by hematoxylin and eosin stain). Five overnight-fasted mice and 5 fed mice with A549 tumors were observed. **Results:** Small-animal PET scans were obtained in fed animals on day 1 and in the same animals after overnight fasting; the lapse was approximately 14 h. Blood glucose concentration after overnight fasting was not different from fed mice ($P = 0.42$), but body weight loss was significant after overnight fasting ($P = 0.001$). Intratumoral distribution of ^{18}F-FDG was highly heterogeneous in all tumors examined, and change in spatial intratumoral distribution of ^{18}F-FDG between 2 sets of PET images from the same mouse was remarkably different in all mice. Tumor ^{18}F-FDG mean SUV and maximum SUV were not significantly different between fed and fasted animals (all $P > 0.05$, $n = 10$). Only tumor mean SUV weakly correlated with blood glucose concentration ($R^2 = 0.17$, $P = 0.03$). In ex vivo studies, in fasted mice, there was spatial colocalization between high levels of ^{18}F-FDG uptake and pimonidazole-binding hypoxic cancer cells; in contrast, pimonidazole-negative normoxic cancer cells and noncancerous stroma were associated with low ^{18}F-FDG uptake. However, high ^{18}F-FDG uptake was frequently observed in noncancerous stroma of tumors but rarely in viable cancer cells of the tumors in fed animals. **Conclusion:** Host dietary status may play a key role in intratumoral distribution of ^{18}F-FDG. In the fed animals, ^{18}F-FDG accumulated predominantly in noncancerous stroma in the tumors, that is, reverse Warburg effect. In contrast, in fasted status, ^{18}F-FDG uptake was found in hypoxic cancer cells component (Pasteur effect). Our findings may provide a better understanding of competing cancer glucose metabolism hypotheses: the Warburg effect, reverse Warburg effect, and Pasteur effect.

Key Words: ^{18}F-fluorodeoxyglucose; reverse Warburg effect; Pasteur effect; PET; non–small cell lung cancer

J Nucl Med 2015; 56:607–612
DOI: 10.2967/jnumed.114.148254

The glucose analog ^{18}F-FDG combined with PET has emerged as an important clinical tool for cancer detection, staging, and monitoring of response and is routinely used in the clinical management of several cancer types. However, the mechanisms involved in ^{18}F-FDG uptake in cancer are not fully understood, and the current literature is mixed and contradictory.

The German chemist and physician Otto Warburg found that Ehrlich ascites cancer cells had increased glucose demand. He observed that even in the presence of ample oxygen, cancer cells prefer to metabolize glucose by aerobic glycolysis due to mitochondrial dysfunction, the so-called Warburg effect (*1*). Increased glucose demand has been considered as one of the fundamental features of cancer (*2*), and this has been exploited clinically for cancer detection by ^{18}F-FDG PET. In operational terms, the Warburg effect increases the relative uptake of ^{18}F-FDG in tumors said to be unrelated to the microdistribution of hypoxia. However, growing evidence indicates that ^{18}F-FDG uptake is significantly higher in hypoxic cancer cells than normoxic cancer cells (*3–11*), and ^{18}F-FDG uptake in the latter is typically low and not statistically different from stromal or necrotic regions (*3*). These findings raise the question of whether the Warburg effect actually applies to normoxic cancer cells (*4*).

We and others have recently documented that hypoxic cancer cells have significantly higher ^{18}F-FDG uptake than aerobic ones in vivo animal studies (*3–7*) as well as in in vitro cell culture studies (*8–11*) in various cancer cell lines. Therefore, in the absence of oxygen, cancer cells seem to have increased demand for glucose or ^{18}F-FDG uptake, and this may be more logically explained by anaerobic glycolysis or the Pasteur effect (*3,4,7*).

On the other hand, Lisanti et al. recently proposed the reverse Warburg effect in a human breast cancer model (*12*). They demonstrated that aerobic glycolysis actually takes place in tumor-associated fibroblasts and not in cancer cells (*12–16*), which challenges the Warburg effect. This reverse Warburg effect hypothesis has not yet been explored in any ^{18}F-FDG study.

Received Sep. 8, 2014; revision accepted Jan. 26, 2015.
For correspondence or reprints contact either of the following:
Xiao-Feng Li, Department of Diagnostic Radiology, University of Louisville, 530 S. Jackson St., CCB-C07, Louisville, KY 40202.
E-mail: linucmed@gmail.com
Xuemei Wang, Department of Nuclear Medicine, Inner Mongolia Medical University Affiliated Hospital, 1 N. Tongdao St., Huimin District, Hohhot, Inner Mongolia, China 010070.
E-mail: wangxuemei201010@163.com
*Contributed equally to this work.
Published online Feb. 26, 2015.
COPYRIGHT © 2015 by the Society of Nuclear Medicine and Molecular Imaging, Inc.

Blood glucose levels of tumor-bearing subjects have been considered as a key factor affecting ^{18}F-FDG uptake in PET studies (*17–21*). Therefore, fasting is a routine procedure in clinical and preclinical studies. Variable effects of fasting on blood glucose levels as well as ^{18}F-FDG uptake have been observed (*17–21*). The effect of changes in blood glucose levels on intratumoral spatial distribution of ^{18}F-FDG is unknown.

In the present study, we used small-animal PET to observe ^{18}F-FDG uptake in the same animals in both fed and fasting states, and ^{18}F-FDG uptake was related to blood glucose levels. We also tested the effect of fasting or feeding on intratumoral spatial ^{18}F-FDG distribution using digital autoradiography and immunohistochemical staining.

MATERIALS AND METHODS

Cancer Cell Line, Nude Mice, and Cancer Models

The human non–small cell lung cancer A549 cell line, purchased from American Type Culture Collection, was used in our experiments. A549 cells were maintained in F-12K medium (American Type Culture Collection) supplemented with 10% fetal bovine serum (Gemini), 1% glutamine, and 1% antibiotic mixture (Cellgro). Cells were grown in a humidified incubator at 37°C in an air atmosphere containing 5% carbon dioxide. Exponentially growing cells were harvested with a 0.25% (w/v) trypsin–0.53 mM ethylenediaminetetraacetic acid solution.

All experiments were performed using 6-wk-old female athymic NCr-*nu/nu* mice purchased from NCI-Frederick Cancer Research Institute. Nude mice were maintained and used according to institutional guidelines. The experimental protocol was approved by the Institutional Animal Care and Use Committee of University of Louisville. Animals were housed 5 per cage and kept in the institutional small-animal facility at a constant temperature and humidity. Food pellets and water were provided ad libitum.

Subcutaneous tumors were initiated by injecting 5×10^6 tumor cells in 0.1 mL of phosphate-buffered saline into each flank of the mouse, and xenografts grew to approximately 1 cm in diameter 3–4 wk later.

Experimental Procedures

Mouse Blood Glucose Measurement. Blood glucose level was measured using an ACCU-CHEK nano glucose meter and ACCU-CHEK SmartView strips (Roche Diagnostics) immediately before each ^{18}F-FDG injection; 2 glucose measurements were taken and the average value was used. Glucose strips were validated using D-glucose water solution (50 and 100 mg/dL), and 5 strips for each concentration were tested; in addition, in a pilot study, 5 measurements were performed in blood from a nude mouse (*21*). The readings by the glucose meter were validated to be accurate.

In Vivo Small-Animal PET Imaging. ^{18}F-FDG was purchased from the P.E.T. NET Pharmaceuticals Inc. facility at University of Louisville Hospital. All animals were imaged prone using the dedicated 3-dimensional small-animal R4 MicroPET (Concorde Microsystems) system. The R4 MicroPET scanner has a transaxial field of view of 10 cm and an axial field of view of 7.8 cm. The resulting list-mode data were sorted into 2-dimensional histograms by Fourier rebinning and the images reconstructed by an iterative reconstruction algorithm into a $128 \times 128 \times 63$ ($0.72 \times 0.72 \times 1.3$ mm) matrix. All animals were fed on day 1, and animals were fasted overnight for the day-2 PET study. Mice were injected without anesthesia via the tail vein with ^{18}F-FDG (9.7 ± 0.3 MBq) and allowed freedom of movement for approximately 60 min. Animals were then anesthetized by inhalation of an isoflurane (1.5%)–air mixture, and a 10-min PET scan was obtained. We included 5 mice with each flank bearing an A549 xenograft (i.e., 2 tumors per mouse) in the small-animal PET study.

PET Image Analysis

Inveon Research Workplace software (version 3.0; Siemens) was used for small-animal PET image analysis. All image sets for each animal were visually examined using a rotating (cine) 3-dimensional display. The window and level settings were adjusted for the best intratumoral distribution visibility. Three-dimensional regions of interest were manually drawn around the edge of the tumor xenograft activity by visual inspection using Inveon Research Workplace for each scan, and the mean and maximal activities were recorded from entire ROIs. The standardized uptake value (SUV) was used to represent tissue ^{18}F-FDG uptake as follows: SUV = region-of-interest activity concentration multiplied by mouse weight divided by injected activity (*21*).

Ex Vivo Autoradiography and Histologic Assay. In a separate group of mice, 5 fasted mice and 5 fed mice (total 10 mice) were included. A mixture of ^{18}F-FDG (7.4 MBq) and pimonidazole (2 mg) was injected via the tail vein 1 h before animal euthanasia (total injection volume, 0.2 mL) as described previously (*3,4*). Blood glucose levels were measured.

As we described previously (*3,4,7,22–24*), immediately after animal sacrifice, tumor tissues were removed for subsequent processing. Subcutaneous xenografts were frozen and embedded in optimal-cutting-temperature medium (Sakura Finetek). Immediately thereafter, 5 contiguous 7-μm-thick tissue sections were cut using a 3050S cryostat microtome (Leica, Inc.) and adhered to poly-L-lysine–coated glass microscope slides (Fisher Scientific, Inc.).

Autoradiograms were obtained by placing the tumor sections in a film cassette against an imaging plate as described previously (*3,4,22*). The same plate was used throughout the experiments; the plate was exposed for approximately 20 h and read by a Cyclone Plus imaging system (PerkinElmer, Inc.). For digital autoradiography, regions of interest (100×100 μm) were drawn over hypoxic cancer cell, oxic cancer cell, and stromal areas, with reference to the immunohistochemical and hematoxylin and eosin stain images obtained from the same or an adjacent section. Digital autoradiography imaging was quantified by OptiQuant software (PerkinElmer Inc.). ^{18}F-FDG uptake was initially expressed as digital light unit per square millimeter and was subsequently converted to MBq/g based on the known section thickness and system calibration factor of 35.4 digital light units per Becquerel (*3*). Finally, ^{18}F-FDG uptake in each microenvironment component was expressed as percentage injected dose per gram of tumor tissue.

To minimize issues associated with section alignment and registration, the same tumor sections used for autoradiography or contiguous adjacent sections were used for all images. Microscopic images of the distributions of pimonidazole and hematoxylin and eosin were obtained from the same or adjacent section as described after completion of autoradiography exposures as reported previously (*3,4,22,24*). Briefly, slides were air-dried, fixed in cold acetone (4°C) for 20 min, and incubated with SuperBlock (Pierce Biotechnology) at room temperature for 30 min. All antibodies were also applied in SuperBlock. Sections were then incubated with fluorescein isothiocyanate–conjugated antipimonidazole monoclonal antibody (Hypoxyprobe Inc.), diluted 1:25, for 1 h at room temperature.

Statistical Analysis

Statistical significance was examined by paired t test and 2-tailed Student t test when appropriate. The paired t test was used when comparing pair data from the same animal. Correlation was analyzed by Pearson correlation using GraphPad Prism (GraphPad Software Inc.). A P value of less than 0.05 was considered statistically significant.

RESULTS

Blood glucose level was measured in 5 mice enrolled in the 2-d PET studies. Changes in blood glucose after overnight fasting were not significant ($P = 0.42$): 93 ± 23 for feeding and 81 ± 35 mg/dL for fasting (Fig. 1A). Body weight was significantly decreased after overnight fasting; animals weighed 23 ± 2 g in the fed status and weight decreased to 20 ± 1 g after overnight fasting ($P = 0.001$) (Fig. 1B). ^{18}F-FDG uptake was expressed as SUV.

PET scans were obtained in 5 mice with an A549 xenograft on each flank. On day 1, a small-animal PET scan was obtained for fed animals. On day 2, a small-animal PET scan was acquired for overnight-fasted animals. The lapse between the 2 sets of PET scans was approximately 14 h. Paired PET images are presented in Figure 2, Figure 3, and Supplemental Figure 1 (supplemental materials are available at http://jnm.snmjournals.org). The intratumoral distribution of ^{18}F-FDG was highly heterogeneous in all tumors examined, and spatial intratumoral distribution of ^{18}F-FDG on day-1 and day-2 PET images from the same mouse was remarkably different in all mice (Figs. 2 and 3; Supplemental Fig. 1). However, overall tumor ^{18}F-FDG mean SUV (SUV_{mean}) was not significantly different between fed (0.45 ± 0.13) and fasted status (0.49 ± 0.20) ($P = 0.50$, $n = 10$) (Fig. 4A), and there was no significant difference in maximum SUV (SUV_{max}) between fed (0.94 ± 0.37) and fasted status (1.02 ± 0.33) ($P = 0.52$) (Fig. 4B).

Although there was weak correlation between tumor SUV_{mean} and blood glucose level ($R^2 = 0.17$, $P = 0.03$) (Fig. 4C), the correlation between tumor SUV_{max} and blood glucose level was not significant ($R^2 = 0.14$, $P = 0.052$) (Fig. 4D). No significant correlation was found between changes in blood glucose concentrations and changes in SUV_{max} or changes in SUV_{mean} (data not shown).

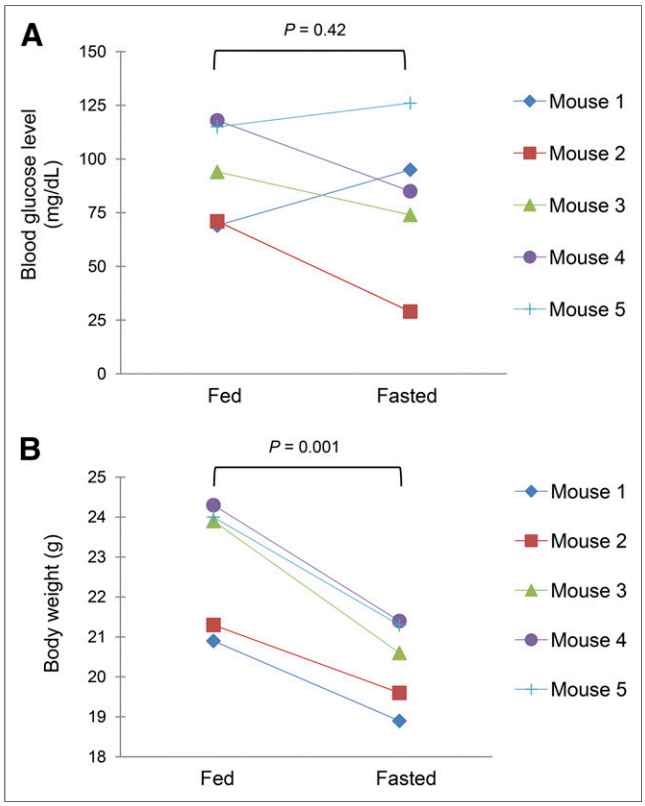

FIGURE 1. Comparison of blood glucose levels (A) and body weights (B) in fed and overnight-fasted mice bearing A549 subcutaneous xenografts ($n = 5$ in both cases).

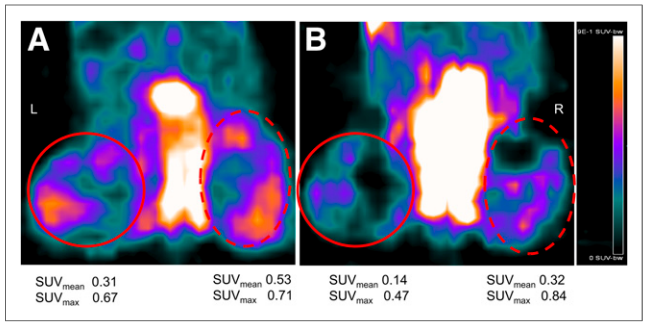

FIGURE 2. Coronal ^{18}F-FDG PET sections of A549 xenograft–bearing mouse-1 in fed (A) and fasted (B) status. Tumors on both flanks are circled. Apparent differences in intratumoral spatial distribution of ^{18}F-FDG was visualized. There is increase in blood glucose level after fasting from 69 mg/dL (fed) to 95 mg/dL.

In a separate experiment, ^{18}F-FDG autoradiography was compared with immunohistochemical/histologic staining visualization of the tumor microenvironment to observe the effect of fasted (in 5 mice) and fed (in 5 mice) status on intratumoral spatial distribution of ^{18}F-FDG in A549 tumors. In A549 xenograft tumors after the host animal was fasted overnight, there was spatial colocalization between high levels of ^{18}F-FDG uptake and pimonidazole binding to hypoxic cancer cells; in contrast, pimonidazole-negative aerobic cancer cells and noncancerous stromal cells showed low ^{18}F-FDG uptake (Fig. 5A). Similar findings have been reported elsewhere (*3,4,7,22*). However, in the fed animals ^{18}F-FDG accumulated predominantly in noncancerous stroma in the tumors, and there was little ^{18}F-FDG uptake in viable cancer cells, regardless of tumor oxygenation status (Fig. 5B; Supplemental Fig. 2). ^{18}F-FDG uptake in stroma significantly increased in fed status, but ^{18}F-FDG accumulation in hypoxic cancer cells significantly decreased, and there was no change in ^{18}F-FDG uptake in oxic cancer cells regardless of feeding or fasting (Fig. 5C). The blood glucose level was 95 ± 34 mg/dL ($n = 5$) for fed mice and 84 ± 31 mg/dL ($n = 5$) for fasted mice ($P > 0.05$). These levels were not statistically different from mice-enrolled PET studies in either fed or fasted status.

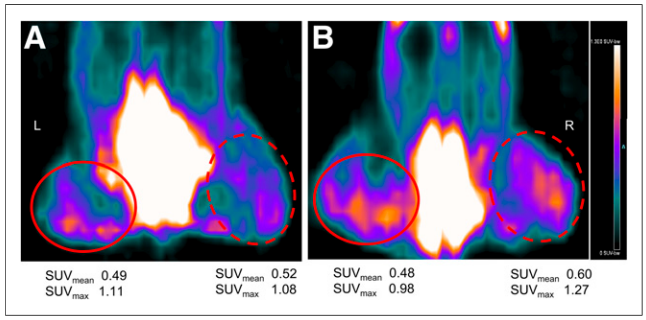

FIGURE 3. Coronal ^{18}F-FDG PET sections of A549 xenograft–bearing mouse-3 in fed (A) and fasted (B) status. Tumors on both flanks are circled. Apparent differences in intratumoral spatial distribution of ^{18}F-FDG were visualized. There is decrease in blood glucose level after fasting from 94 mg/dL (fed) to 74 mg/dL.

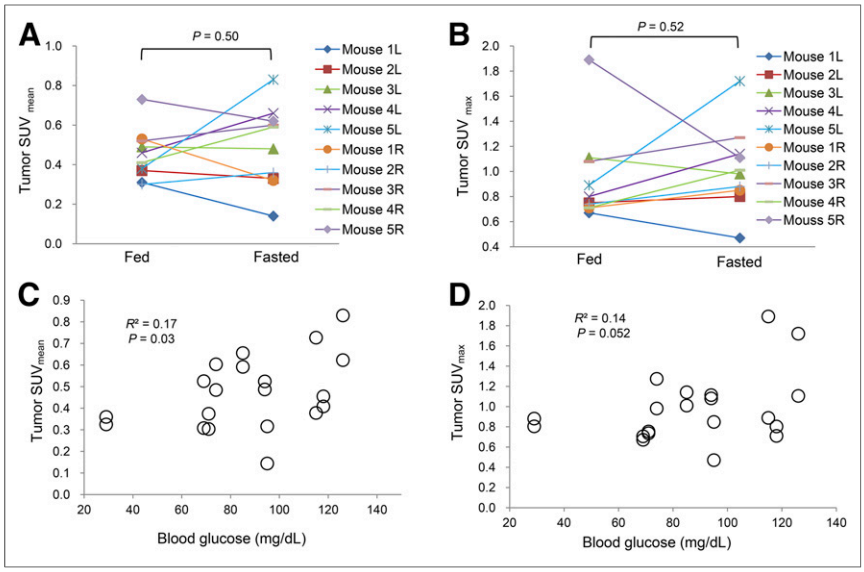

FIGURE 4. (A) Comparison of tumor SUV_{mean} between fed and fasting status in 5 mice bearing A549 tumors. (B) Comparison of tumor SUV_{max} between fed and fasted status. There was no significant difference in SUV_{max} between fed (0.94 ± 0.37) and fasted status (1.02 ± 0.33) (P = 0.52). (C) Correlation between tumor SUV_{mean} and blood glucose levels. (D) Correlation between tumor SUV_{max} and blood glucose levels.

DISCUSSION

^{18}F-FDG PET is routinely used in the clinical management of cancers, and its utility is usually thought to be due to enhanced aerobic glycolysis in tumors—that is, the Warburg effect. Increased glucose metabolism has been considered a fundamental feature of cancer. However, the Warburg effect hypothesis has been challenged in several ways.

First, we have documented that the Ehrlich ascites cells, which Warburg used, were severely hypoxic, and glucose demand measured by ^{18}F-FDG uptake was high (*4,7*). Ascites cancer cells may use anaerobic glycolysis (Pasteur effect) to generate adenosine triphosphate. The higher uptake of ^{18}F-FDG in hypoxic ascites cancer cells may be explained by the Pasteur effect (low oxygen tension and high glucose utilization) not aerobic glycolysis (high oxygen and high glucose utilization; the Warburg effect) (*4*).

Second, multiple studies have recently documented that hypoxic cancer cells have significantly higher ^{18}F-FDG uptake than aerobic ones (Fig. 4A) (*3–11*). Therefore, high glucose demand may be a general feature of hypoxic cancer cells not normoxic ones.

Third, Lisanti et al. have recently proposed the reverse Warburg effect. On the basis of their observations in human breast cancers, they concluded that so-called aerobic glycolysis actually takes place in tumor-associated fibroblasts not in cancer cells (*12–16*). Here, we found that in fed mice, intratumoral high ^{18}F-FDG activity was predominantly associated with noncancerous stroma and neither hypoxic nor aerobic cancer cells showed higher ^{18}F-FDG uptake (Figs. 5B and 5C; Supplemental Fig. 2). Accordingly, we hypothesized that, under fed status, intratumoral stroma adjacent to functional blood vessels use most glucose supplied by the circulation, whereas viable cancer cells do not, which may be explained by the reverse Warburg effect. In contrast, ^{18}F-FDG uptake was predominantly found in hypoxic cancer cells in tumor-bearing animals in the fasted condition (Figs. 5A and 5C). Similar results have been observed by us and others (*3–7*). Therefore, host dietary status may play a key role in intratumoral distribution of ^{18}F-FDG.

In a group of 5 mice, we found blood glucose levels did not significantly change after overnight fasting; however, animal body weight was significantly decreased by an average of 3 g after 14-h fasting (Fig. 1). This decrease in body weight can be explained by the fact that animals self-regulate to keep glucose levels constant using stored energy sources or gluconeogenesis. It is not surprising that ^{18}F-FDG uptake measured by small-animal PET was not changed in the tumors (Fig. 4).

In general, blood glucose level has been considered a key factor affecting ^{18}F-FDG PET imaging. Our PET findings indicated that tumor ^{18}F-FDG SUV_{mean} had weak correlation with blood glucose level (R^2 = 0.17, P = 0.03), but ^{18}F-FDG SUV_{max} did not correlate with blood glucose level (Figs. 4C and 4D). In addition, changes in tumor ^{18}F-FDG uptake did not correlate with changes in glucose levels. Our data indicate that blood glucose level may not be the major factor affecting ^{18}F-FDG SUV in cancer-growing mice without documented glucose metabolism abnormalities.

There is apparent discrepancy in tumor ^{18}F-FDG uptake between patients and mice. Tumor ^{18}F-FDG uptake in nonfasted patients generally is much reduced, compared with the fasted case; however, there were no significant changes in tumor uptake between fasted and nonfasted states in mice. The mechanism inducing the apparent discrepancy is unclear, but difference in stroma between mice and humans may play a role.

In ex vivo studies using autoradiography–immunohistochemical assays, we observed ^{18}F-FDG uptake in each component of the tumor. Apparently higher ^{18}F-FDG accumulation may have shifted from hypoxic cancer cells to stroma components in the fed state (Fig. 5; Supplemental Fig. 2). Therefore, the PET findings of change in spatial intratumoral distribution of ^{18}F-FDG between fed and fasted status can be explained. SUVs reflect the entire tumor level, and spatial changes in ^{18}F-FDG distribution among tumor microenvriomental components may not necessarily alter overall ^{18}F-FDG uptake. Our findings presented in Figure 4 are not contradicted by autoradiography–immunohistochemical findings (Fig. 5; Supplemental Fig. 2) and PET images (Figs. 2 and 3). In clinical settings, it is important to observe intratumoral distribution of ^{18}F-FDG in addition to SUV in serial PET/CT studies to manage cancer therapy in oncology patients.

In this study, we used SUV instead of percentage injected dose per gram to present ^{18}F-FDG uptake. We chose the SUV parameter because animal body weight significantly changed, and the body weight factor has to be considered for accurate data presentation.

Our study has the following limitations: the lapse between the 2 sets of PET scans was approximately 14 h, slightly over 7 half-lives decay for ^{18}F. This time was chosen to minimize the residual radioactivity effect remaining from the first injection into the second imaging. Residual ^{18}F-FDG from the first PET study was considered completely decayed. And the overnight fasting frequently

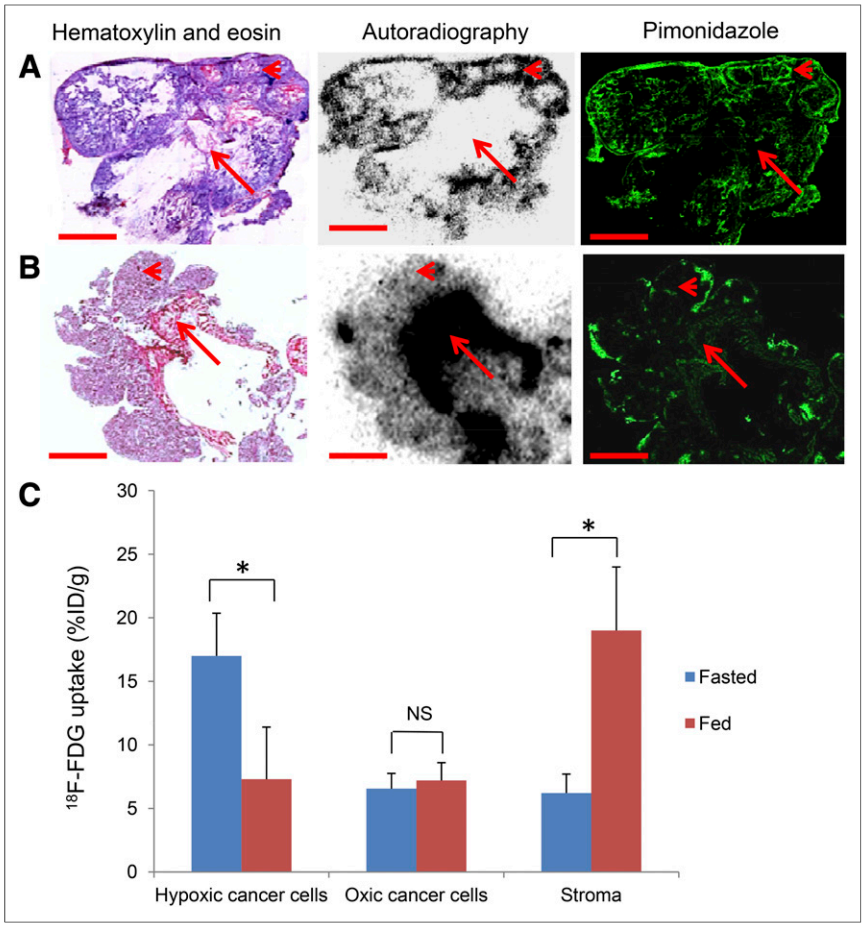

FIGURE 5. Comparison of intratumoral distribution of ^{18}F-FDG by autoradiography with immunohistochemical–histologic staining visualization of microenvironment components in A549 tumors. (A) Fasted status. There was spatial colocalization between high levels of ^{18}F-FDG uptake and pimonidazole binding (green) in hypoxic cancer cells (arrowhead). Noncancerous stroma was associated with low ^{18}F-FDG uptake (arrow); blood glucose level of mouse was 79 mg/dL. (B) In fed animal with blood glucose level of 114 mg/dL, ^{18}F-FDG accumulated predominantly in noncancerous stroma in tumor (arrow), and there was little ^{18}F-FDG uptake in viable cancer cells whether stained positively or negatively for pimonidazole (arrowhead). (C) ^{18}F-FDG uptake (percentage injected dose per gram [%ID/g]) in each microenvironment component. *$P < 0.001$, n = 10–20 measurements from 5 tumors. All scale bars = 2 mm. NS = not significant.

mimics patients' situations in clinical PET studies wherein they are required to fast for at least 6 h. Published data have documented that the tumor microenvironment may change over short periods of time in some cancer types (*25,26*). Our published results confirmed that an A549 xenograft tumor microenvironment is mostly stable during a 10- to 14-h time interval (*22*). Paired PET studies were also conducted in 2 fasted mice with A549 tumors within 14 h, and intratumoral distribution of ^{18}F-FDG was highly reproducible (data not shown). Thus, demonstrated mismatch patterns of ^{18}F-FDG PET images between fasted and fed status were valid and not the consequence of significant spatial change in the intratumoral microenvironment.

Animal body weight significantly decreased after overnight fasting, but glucose levels were not different from fed status. Apparently the prolonged fasting puts animals into a condition of metabolic stress. A drop in blood glucose leave was expected but not found; stress-triggered homeostatic responses generate more new glucose to keep blood glucose more or less constant. A short period of fasting should be observed in a future study.

Host dietary status may play a key role in intratumoral distribution of ^{18}F-FDG. However, insulin and other hormone levels and their effects on ^{18}F-FDG uptake were not included in the present study, and future investigations may need to explore these important issues in other cancer cell lines.

CONCLUSION

In this study, host dietary status may play a key role in intratumoral distribution of ^{18}F-FDG. In the fed animals, ^{18}F-FDG accumulated predominantly in noncancerous stroma in the tumors—that is, reverse Warburg effect. The effect of blood glucose level on ^{18}F-FDG uptake in A549 tumors was minimal. Our findings may provide a better understanding of 3 competing intratumoral glucose metabolism hypotheses: the Warburg effect, reverse Warburg effect, and Pasteur effect.

DISCLOSURE

The costs of publication of this article were defrayed in part by the payment of page charges. Therefore, and solely to indicate this fact, this article is hereby marked "advertisement" in accordance with 18 USC section 1734. This study was supported by the Kentucky Lung Cancer Research program award (cycle 9), Inner Mongolia Natural Science Foundation awards (2012MS1153, 2014MS0835, and 2014MS0859), and National Natural Science Foundation of China award (81360227). No other potential conflict of interest relevant to this article was reported.

ACKNOWLEDGMENTS

We thank Dr. John Eaton from University of Louisville for critically reading the manuscript and Dr. Haixun Guo for technical supports of PET studies.

REFERENCES

1. Warburg O. On the origin of cancer cells. *Science.* 1956;123:309–314.
2. Vander Heiden MG, Cantley LC, Thompson CB. Understanding the Warburg effect: the metabolic requirements of cell proliferation. *Science.* 2009;324:1029–1033.
3. Huang T, Civelek AC, Li J, et al. Tumor microenvironment-dependent ^{18}F-FDG, ^{18}F-fluorothymidine, and ^{18}F-misonidazole uptake: a pilot study in mouse models of human non-small cell lung cancer. *J Nucl Med.* 2012;53:1262–1268.
4. Li XF, Du Y, Ma Y, et al. ^{18}F-fluorodeoxyglucose uptake and tumor hypoxia: Revisit ^{18}F-fluorodeoxyglucose in oncology application. *Transl Oncol.* 2014;7:240–247.
5. Pugachev A, Ruan S, Carlin S, et al. Dependence of FDG uptake on tumor microenvironment. *Int J Radiat Oncol Biol Phys.* 2005;62:545–553.
6. Busk M, Horsman MR, Kristjansen PE, van der Kogel AJ, Bussink J, Overgaard J. Aerobic glycolysis in cancers: implications for the usability of oxygen-responsive

genes and fluorodeoxyglucose-PET as markers of tissue hypoxia. *Int J Cancer.* 2008;122:2726–2734.
7. Li XF, Ma Y, Sun X, Humm JL, Ling CC, O'Donoghue JA. High ^{18}F-FDG uptake in microscopic peritoneal tumors requires physiological hypoxia. *J Nucl Med.* 2010;51:632–638.
8. Clavo AC, Brown RS, Wahl RL. Fluorodeoxyglucose uptake in human cancer cell lines is increased by hypoxia. *J Nucl Med.* 1995;36:1625–1632.
9. Burgman P, O'Donoghue JA, Humm JL, Ling CC. Hypoxia-induced increase in FDG uptake in MCF7 cells. *J Nucl Med.* 2001;42:170–175.
10. Hara T, Bansal A, DeGrado TR. Effect of hypoxia on the uptake of [methyl-^{3}H] choline, [1-^{14}C] acetate and [^{18}F]FDG in cultured prostate cancer cells. *Nucl Med Biol.* 2006;33:977–984.
11. Busk M, Horsman MR, Jakobsen S, Bussink J, van der Kogel A, Overgaard J. Cellular uptake of PET tracers of glucose metabolism and hypoxia and their linkage. *Eur J Nucl Med Mol Imaging.* 2008;35:2294–2303.
12. Pavlides S, Whitaker-Menezes D, Castello-Cros R, et al. The reverse Warburg effect: aerobic glycolysis in cancer associated fibroblasts and the tumor stroma. *Cell Cycle.* 2009;8:3984–4001.
13. Pavlides S, Tsirigos A, Vera I, et al. Transcriptional evidence for the "reverse Warburg effect" in human breast cancer tumor stroma and metastasis: similarities with oxidative stress, inflammation, Alzheimer's disease, and "neuron-glia metabolic coupling." *Aging (Albany NY).* 2010;2:185–199.
14. Bonuccelli G, Whitaker-Menezes D, Castello-Cros R, et al. The reverse Warburg effect: glycolysis inhibitors prevent the tumor promoting effects of caveolin-1 deficient cancer associated fibroblasts. *Cell Cycle.* 2010;9:1960–1971.
15. Pavlides S, Tsirigos A, Vera I, et al. Loss of stromal caveolin-1 leads to oxidative stress, mimics hypoxia and drives inflammation in the tumor microenvironment, conferring the "reverse Warburg effect": a transcriptional informatics analysis with validation. *Cell Cycle.* 2010;9:2201–2219.
16. Martinez-Outschoorn UE, Pavlides S, Whitaker-Menezes D, et al. Tumor cells induce the cancer associated fibroblast phenotype via caveolin-1 degradation: implications for breast cancer and DCIS therapy with autophagy inhibitors. *Cell Cycle.* 2010;9:2423–2433.
17. Lindholm P, Minn H, Leskinen-Kallio S, Bergman J, Ruotsalainen U, Joensuu H. Influence of the blood glucose concentration on FDG uptake in cancer: a PET study. *J Nucl Med.* 1993;34:1–6.
18. Crippa F, Gavazzi C, Bozzetti F, et al. The influence of blood glucose levels on [^{18}F]fluorodeoxyglucose (FDG) uptake in cancer: a PET study in liver metastases from colorectal carcinomas. *Tumori.* 1997;83:748–752.
19. Rabkin Z, Israel O, Keidar Z. Do hyperglycemia and diabetes affect the incidence of false-negative ^{18}F-FDG PET/CT studies in patients evaluated for infection or inflammation and cancer? A comparative analysis. *J Nucl Med.* 2010;51:1015–1020.
20. Sha W, Ye H, Iwamoto KS, et al. Factors affecting tumor ^{18}F-FDG uptake in longitudinal mouse PET studies. *EJNMMI Res.* 2013;3:51.
21. Dandekar M, Tseng JR, Gambhir SS. Reproducibility of ^{18}F-FDG microPET studies in mouse tumor xenografts. *J Nucl Med.* 2007;48:602–607.
22. Li XF, Huang T, Jiang H, et al. Combination of ^{18}F-fluorodeoxyglucose and ^{18}F-fluorothymidine PET achieves more complete identification of viable cancer cells in lung cancer of the mouse and the patient than individual radiopharmaceutical: A proof-of-concept study. *Transl Oncol.* 2013;6:775–783.
23. Li XF, Sun X, Ma Y, et al. Detection of hypoxia in microscopic tumors using ^{131}I-labeled iodoazomycin galactopyranoside (^{131}I-IAZGP) digital autoradiography. *Eur J Nucl Med Mol Imaging.* 2010;37:339–348.
24. Li XF, Carlin S, Urano M, Russell J, Ling CC, O'Donoghue JA. Visualization of hypoxia in microscopic tumors by immunofluorescent microscopy. *Cancer Res.* 2007;67:7646–7653.
25. Ljungkvist AS, Bussink J, Kaanders JH, et al. Hypoxic cell turnover in different solid tumor lines. *Int J Radiat Oncol Biol Phys.* 2005;62:1157–1168.
26. Nehmeh SA, Lee NY, Schröder H, et al. Reproducibility of intratumor distribution of ^{18}F-fluoromisonidazole in head and neck cancer. *Int J Radiat Oncol Biol Phys.* 2008;70:235–242.